THE ASTROPHYSICAL JOURNAL, 410:202–217, 1993 June 10

FROM BIPOLAR TO QUADRUPOLAR: THE COLLIMATION PROCESSES OF THE CEPHEUS A OUTFLOW

JOSÉ M. TORRELLES,[1,2] LOURDES VERDES-MONTENEGRO,[1] PAUL T. P. HO,[2]
LUIS F. RODRÍGUEZ,[3] AND JORGE CANTÓ[3]
Received 1992 October 5; accepted 1992 December 11

ABSTRACT

We present new high-angular ($\sim 2''$) and -velocity (~ 0.3 km s^{-1}) resolution observations in the (J, K) = (1, 1) and (2, 2) ammonia lines toward Cepheus A using the VLA D-configuration. As previously reported, the high-density gas is mainly distributed in three clumps, Cep A-1, Cep A-2, and Cep A-3. Cep A-1 and Cep A-3 constitute an interstellar elongated structure ($\sim 2'.3 \times 0'.4$, or $\sim 0.5 \times 0.08$ pc), with the stellar activity center located at its northwest edge. We find that Cep A-1 and Cep A-3 are located, respectively, between the two main pairs of the blue- and redshifted CO lobes of the quadrupolar molecular outflow. This implies that the interstellar disklike structure cannot collimate the bipolar outflow near its origin in the east-west direction. The high-velocity outflow and the photons of its powering source seem to be producing significant perturbations of the morphological, kinematical, and temperature structures at the edges of the ammonia condensations. We suggest that the interstellar high-density condensations are *diverting* and *redirecting* the molecular outflow at scales of ~ 0.05–0.5 pc, with Cep A-1 and Cep A-3 splitting in two halves, respectively, the blue- and redshifted lobes of an originally bipolar outflow already collimated in the east-west direction at circumstellar scales. Part of the high-density gas located at the edges of the interstellar ammonia condensations may be in the process of being incorporated into the general high-velocity molecular outflow by a dragging effect. However, the overall observed motions in the interstellar high-density gas could be bound by the observed mass in the region.

HW 2 is embedded in a circumstellar ($\sim 3''.3 \times 2''.3$, or $\sim 2400 \times 1700$ AU; p.a. = 22°) high-density [$n(H_2) \simeq 3 \times 10^7 (X_{NH_3}/10^{-8})^{-1}$ cm^{-3}] clump of $\sim 2 (X_{NH_3}/10^{-8})^{-1}$ $M_\odot$. The high rotational temperatures [$T_R(22\text{–}11) = 40$–50 K] and the large velocity dispersions in the ammonia emission ($\sigma \simeq 3$–4 km s^{-1}) found toward this position lead us to favor this object as the powering source of the high-velocity outflow. The observed motions of the circumstellar molecular gas could reflect the bound motions of the gas (e.g., rotation or infall) around a central mass of ~ 10–20 $M_\odot$, or alternatively the perturbation of the gas by the wind of the central source. This circumstellar clump could be related to the circumstellar disk previously suggested from infrared continuum and maser line observations.

We find that gas temperatures as a function of the projected distance r with respect to HW 2 can be fitted by $T_R(22\text{–}11) \propto r^{-\alpha}$, with $\alpha = 0.3$–0.6. These indices are quite similar to those expected if heating of the molecular gas is via collisions with hot dust heated by the radiation of the central star(s). The observed luminosity in the region is enough to heat the gas up to the observed temperatures. This analysis suggests that similar VLA studies of radial temperature profiles in other star-forming regions may be very useful for understanding heating processes and identifying exciting sources.

Subject headings: H II regions — ISM: individual (Cepheus A) — ISM: jets and outflows — ISM: molecules

1. INTRODUCTION

Cepheus A is the densest component of the molecular cloud complex associated with Cepheus OB3, which is located at a distance of 725 pc (Johnson 1957). First studied by Sargent (1977) in CO($J = 1$–0) and ^{13}CO($J = 1$–0), the observations in the rarer isotope (beam $\simeq 2'.5$) revealed a molecular structure of ~ 6 pc elongated in the northeast-southwest direction, coinciding with the direction of the Cepheus OB3 complex and the Galactic plane. Rodríguez, Ho, & Moran (1980), with CO($J = 1$–0) observations (beam $\simeq 1'$), detected a bipolar outflow oriented almost perpendicular to the ^{13}CO structure. However, very recent high angular resolution CO($J = 1$–0) observations (beam $\simeq 15''$), carried out by Bally & Lane (1991, 1992), have revealed a much more complex morphology for the outflow, with the more intense blue- and redshifted lobes split in two halves constituting a quadrupolar structure. In order to study the denser gas environment of the outflow, Ho, Moran, & Rodríguez (1982) made single-dish observations of ammonia (beam $\simeq 1'.5$) and detected a condensation of ~ 0.8 pc, elongated in the same direction as the ^{13}CO structure. Most of the single-dish ammonia emission comes from three condensations, Cep A-1, Cep A-2, and Cep A-3, which were detected with the Very Large Array (VLA) in the NH_3(1, 1) and (2, 2) lines (beam $\simeq 10''$; Torrelles et al. 1985, 1986, hereafter THRC85, -86).

Two active zones of star formation have been identified in Cepheus A: Cep A-east and Cep A-west. Both zones are clearly delimited by centimeter continuum observations (Hughes & Wouterloot 1982; Rodríguez & Cantó 1983). Cep A-west, located $\sim 1'.5$ west of Cep A-east, contains the diffuse object

[1] Instituto de Astrofísica de Andalucía, CSIC, Ap. Correos 3004, C/Sancho Panza S/N, E-18080 Granada, Spain.
[2] Harvard-Smithsonian Center for Astrophysics, 60 Garden Street, Cambridge, MA 02138.
[3] Instituto de Astronomía, UNAM, Ap. Postal 70-264, 04510 México, D. F., México.

GGD 37 (Gyulbudaghian, Glushkov, & Denisyuk 1978). This object has been identified as a Herbig-Haro (HH) object (Hartigan & Lada 1985; Hartigan et al. 1986) associated with radio continuum emission (Hughes 1989; Hughes & Moriarty-Schieven 1990).

The molecular outflow is well centered on Cep A-east (Rodríguez et al. 1980; Bally & Lane 1991, 1992). This region contains an infrared source with a luminosity of $\sim 2.5 \times 10^4$ $L_\odot$ (e.g., Evans et al. 1981; Lenzen, Hodapp, & Solf 1984). Corcoran (1991) has recently found a ring of intense [S II] line emission $\sim 1\farcm5$ east of the center of the molecular outflow, which has been interpreted as HH-like emission originated in the walls of a cavity of the outflow. Hughes & Wouterloot (1984) found in Cep A-east 14 continuum sources at cm wavelengths, named as sources HW. We found (THRC85, -86) that these radio sources are mainly located at the edges of the VLA ammonia condensations. We also observed (THRC86) an increase of gas temperatures toward the position of the OH and H_2O masers detected by Norris (1980) and Lada et al. (1981), respectively. On the basis of these observations, we proposed (THRC86) that the radio continuum emission of the HW sources located at the edges of the ammonia condensations corresponds to material externally ionized by two B1 stars, probably located at the position of the OH and H_2O masers. The northern group of H_2O masers (Lada et al. 1981) coincides with the source HW 2, while the southern group of H_2O masers coincides with HW 3d. CS($J = 7$–6) observations carried out by Moriarty-Schieven, Snell, & Hughes (1991) with $\sim 16''$ resolution show also warm ($T_K > 30$ K) high-density [$n(H_2) > 10^6$ cm^{-3}] gas toward the region around HW 2. Cohen, Rowland, & Blair (1984), from their study of radial velocities of the OH and H_2O masers, concluded that the outflow is collimated in the east-west direction, very close to HW 2 ($\leq 10^{15}$ cm). Furthermore, Lenzen et al. (1984), Joyce & Simon (1986), and Lenzen (1988), from near-infrared observations, found an extinction strip near HW 2, suggesting the presence of a circumstellar disk seen almost edge-on. Therefore, taking into account all these observational results, in this paper we shall refer to the region close to HW 2 as the stellar activity center of Cepheus A-east.

Even after the numerous studies on Cepheus A, the relationship between the high-velocity molecular outflow and the ambient cloud remains unclear. Based on our previous VLA-D observations of ammonia (beam $\simeq 10''$, velocity resolution $\simeq$0.6–1.5 km s^{-1}; THRC85, -86), we suggested that Cep A-1, Cep A-2, and Cep A-3 may play an important role in focusing the bipolar outflow in the region. In particular, we proposed (THRC86) that Cep A-1 and Cep A-3 constitute a dense rotating interstellar disk, with a flat rotation curve to within $15''$ from the stellar activity center. We found (THRC86) an important ammonia line broadening ($\Delta V \simeq 4$ km s^{-1}) toward the activity center ($\leq 15''$), which was interpreted as material rotating at higher velocities closer in to a central mass (e.g., Keplerian motions), or, alternatively, due to a perturbation of the molecular gas produced by the stellar wind(s) of the central source(s). We also suggested that the location of the stellar activity center at the northwest edge of the interstellar disklike structure could explain why the CO outflow observed by Rodríguez et al. (1980) expands more freely in the northwest direction, while the outflow in the southeast direction is completely stopped by the dense structure.

In this paper we present further studies on Cepheus A. Taking advantage of the higher sensitivity of the new K-band receivers of the VLA system we have carried out new observations of the (1, 1) and (2, 2) ammonia lines. Our goals were the following: (1) To study fainter structures in the ammonia condensations in order to better define the morphological features which might be shaped by the outflow, as well as to study more precisely the role of the dense gas in the collimation processes of the molecular outflow. (2) To achieve with 0.3 km s^{-1} of velocity resolution a better definition of the kinematics of the high-density gas, in order to analyze, for example, possible Keplerian motions close to the central source. (3) To study the effect of the powering source of the outflow on the dense gas in terms of heating and broadening of the lines.

2. SYSTEM PARAMETERS AND DATA ANALYSIS

Observations of the (1, 1) and (2, 2) rotation-inversion transitions of NH_3 ($\lambda \simeq 1.3$ cm) were made with the VLA of the National Radio Astronomy Observatory (NRAO)[4] in the D-configuration during 1989 November 26. We used the 2AD spectral line mode, which allowed simultaneous observations of the NH_3(1, 1) and NH_3(2, 2) lines. We used for each line a bandwidth of 3.125 MHz. We selected the central 63 spectral channels of the bandwidth, with a spectral resolution of 24.4 kHz ($\sim$0.3 km s^{-1} at $\lambda = 1.3$ cm), plus a continuum channel which contains the average of the central 75% of the 3.125 MHz bandwidth. The center channel LSR velocity was set at -11.15 km s^{-1}. The total observed velocity range ($-21 \lesssim V_{LSR} \lesssim -2$ km s^{-1}) covers the main quadrupole hyperfine component for both ammonia lines and the inner satellite lines for the (1, 1) transition (see Ho & Townes 1983). We used 3C 286 for flux calibration, assuming a flux density S_ν(1.3 cm) = 2.42 Jy. The phase calibrator was 2200+420, with a bootstrapped flux S_ν(1.3 cm) = 4.72 $\pm$ 0.12 Jy. From phase noise, we estimate that our absolute positions are accurate to 10% of the synthesized beams. The phase center of the array was set at $\alpha(1950) = 22^h54^m19\fs10$, $\delta(1950) = 61°45'46\farcs0$. At $\lambda = 1.3$ cm the primary beam size at full width half-maximum (FWHM) is $\sim 2'$.

The data were edited and calibrated using the tasks of the Astronomical Image Processing System (AIPS) software of NRAO. Maps of each spectral line channel were made with uniform and natural weighting. The resulting synthesized beam sizes are $2\farcs4 \times 2\farcs2$ (p.a. = $-29°$, uniform weighting) and $3\farcs4 \times 3\farcs3$ (p.a. = $-40°$, natural weighting). Cleaned maps were obtained with the task MX of AIPS. In order to improve the cleaning of extended structures we have added to the (u, v) data a zero spacing flux density of 20 Jy, estimated from the NH_3 single-dish data of Ho et al. (1982), and Güsten, Chini, & Neckel (1984). We gave this flux a weight of 15, corresponding to the missing 15 cells in the inner region of the (u, v) plane. With this correction we were able to remove the deep negative sidelobes from the original maps. We note that the final maps are not very sensitive to the particular value of zero spacing flux and weight that we used. An rms noise level of ~ 10 mJy (1 σ) per channel for each ammonia line was achieved after 210 minutes of on-source integration. This sensitivity is a factor of $\sim$4–6 higher than that obtained in our previous observations (THRC85, -86). Higher sensitivity to spatially extended low-brightness emission was achieved by convolving the (u, v) data with a Gaussian tapering function of 40 kλ (0.52 km half-width at 30%) and natural weighting. The resulting synthesized beam

[4] The NRAO is operated by Associated Universities, Inc., under cooperative agreement with the National Science Foundation.

size is 5″.4 × 5″.3 (p.a. = −54°). All the maps shown in this paper have been obtained with this synthesized beam. Correction for the primary beam attenuation away from the phase center has not been applied to our maps. The average of the line-free channels has been subtracted from all the individual channels in order to remove the continuum emission from the central H II regions.

3. RESULTS

3.1. $NH_3(1, 1)$ *and* (2, 2) *Emission*

The main component of the $NH_3(1, 1)$ and $NH_3(2, 2)$ transitions is detected in the velocity range $-13 \lesssim V_{LSR} \lesssim -6$ km s^{-1}. The inner satellite lines of the (1, 1) transition were also detected. In Figure 1 we show selected individual channel

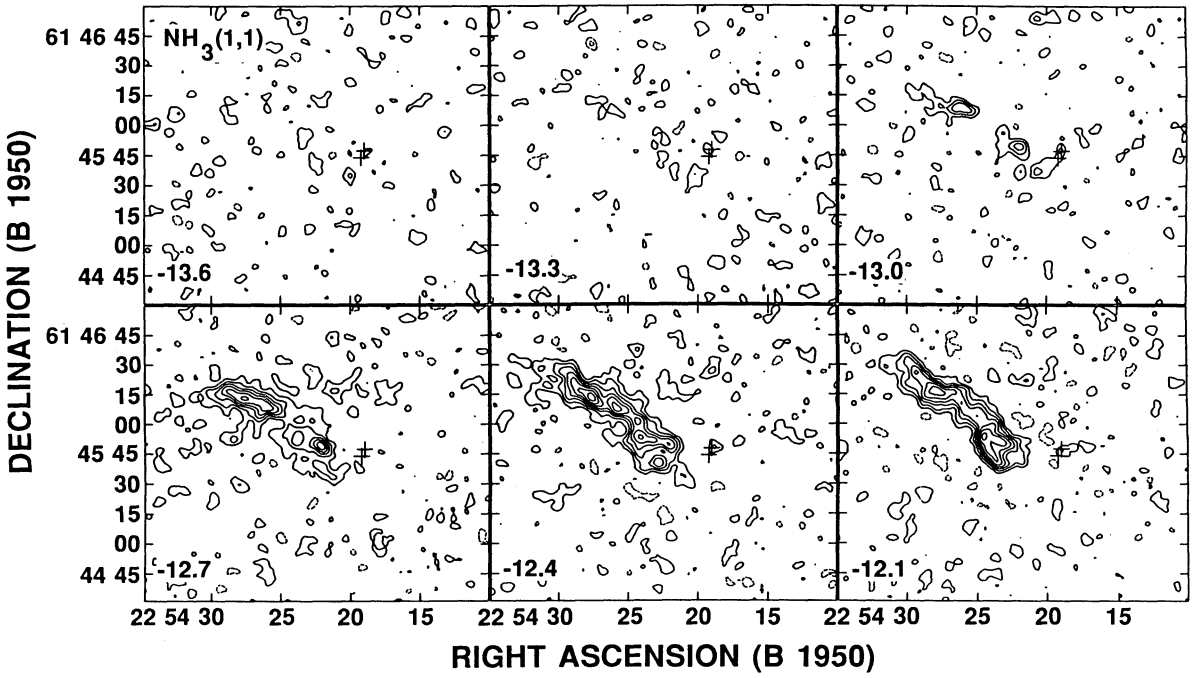

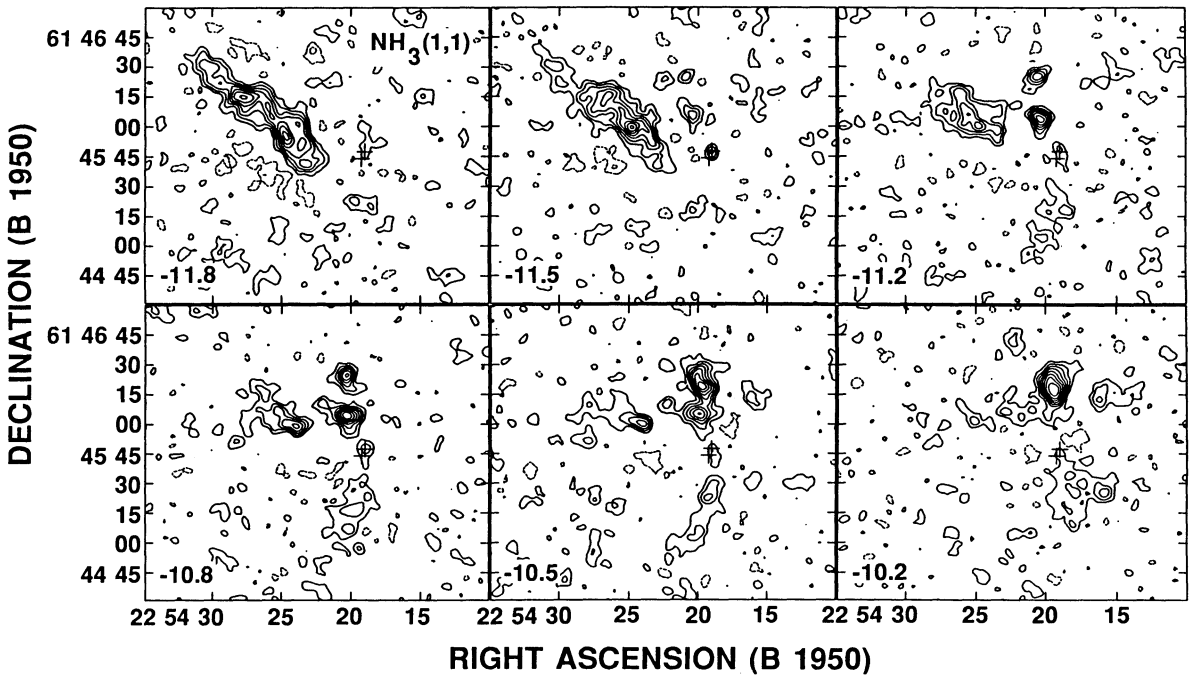

FIG. 1*a*

FIG. 1.—Channel maps of the $NH_3(1, 1)$ (*a*) and $NH_3(2, 2)$ (*b*) emission. The V_{LSR}(km s^{-1}) is indicated. Contours are −4, −2, 2, 4, 6, 8, 10, 12, 14, 16 times 10 mJy beam^{-1}, the rms noise of the maps. Synthesized beam = 5″.4 × 5″.3 (p.a. = −54°). Crosses indicate the position of the H_2O masers (Lada et al. 1981).

contour maps of the main component of the (1, 1) and (2, 2) ammonia lines. The positions of the H_2O masers (Lada et al. 1981) are indicated in all these channel maps by crosses. In Figure 2 we present the $NH_3(1, 1)$ and $NH_3(2, 2)$ spectra observed toward several peaks of the ammonia condensations, at the positions given in Table 1. Typical line widths in the condensations are found to be ~ 1 km s^{-1}. However, remarkably large line widths in both the (1, 1) and (2, 2) lines ($\Delta V \simeq 7$ km s^{-1}) are found toward HW 2 (see Fig. 3).

With higher sensitivity and also higher angular and spectral resolutions than previously reported by THRC85 and THRC86 the structure of the ammonia clumps is defined with much greater details revealing substantially more complexity. New interesting features, with arclike shapes at the edges of the

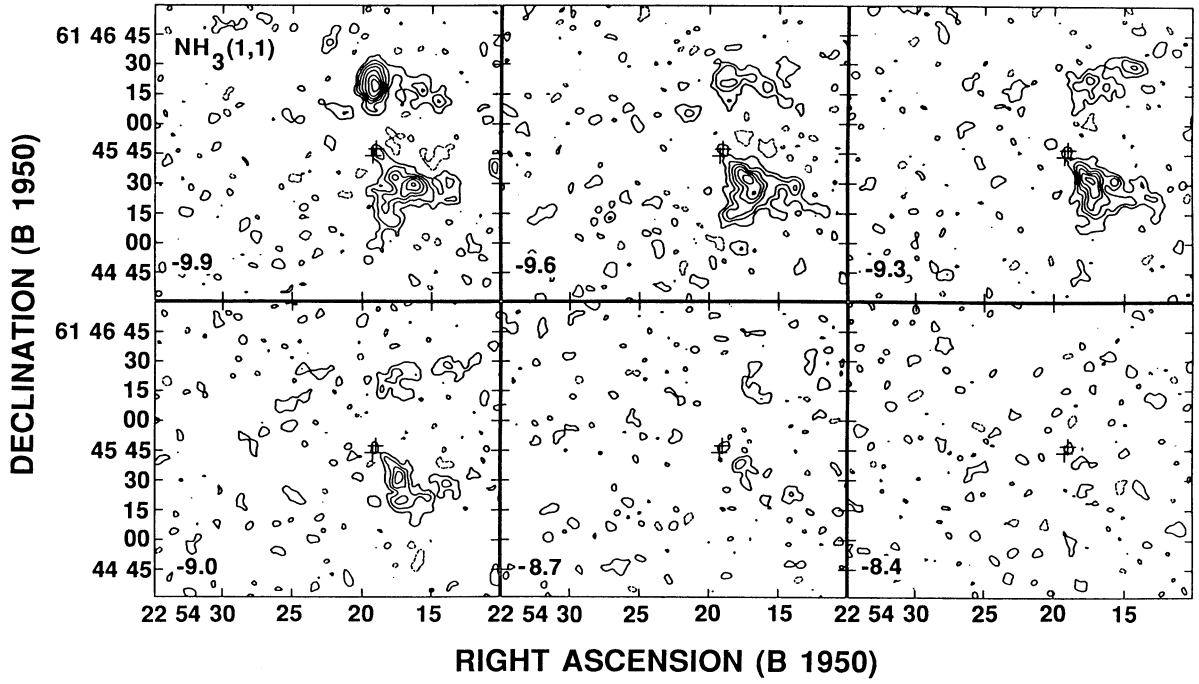

FIG. 1*a*

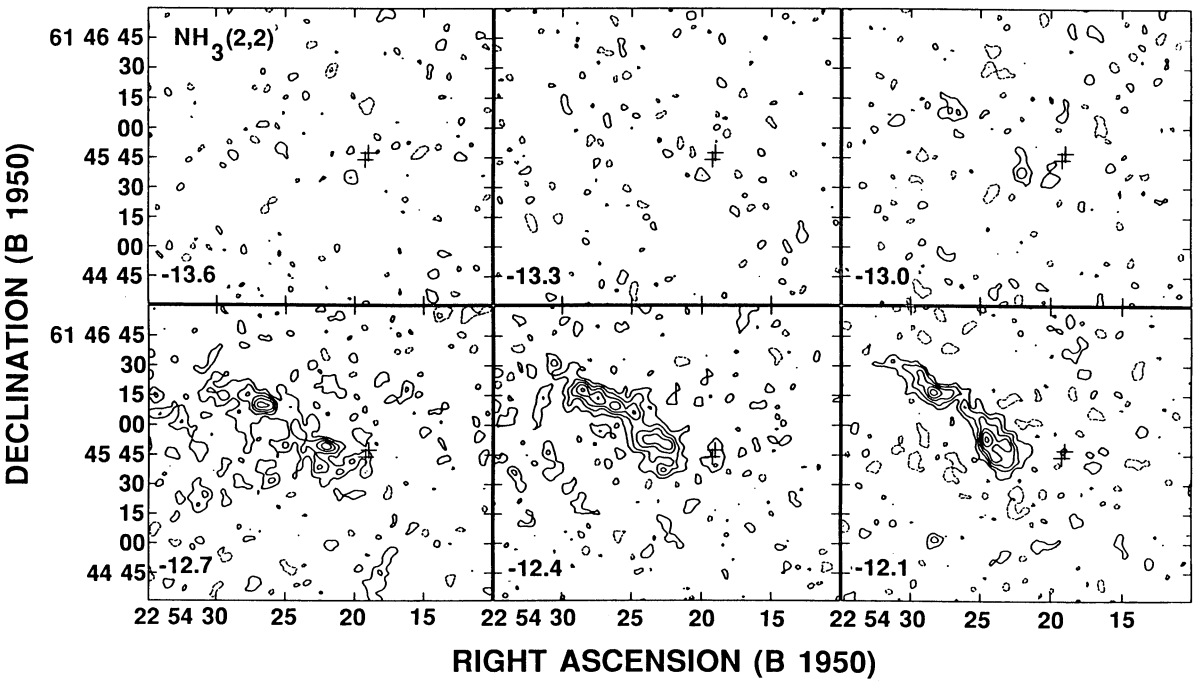

FIG. 1*b*

clumps of Cep A-1 and Cep A-2 and undulations along Cep A-3, have been detected (see below and § 4.1). A new condensation undetected in THRC85 and THRC86 is also now observed in the velocity range $-10.5 \lesssim V_{LSR} \lesssim -11.5$ km s^{-1}, at $\alpha(1950) = 22^h54^m20^s.23$, $\delta(1950) = 61°46'05''.0$ (see Fig. 1).

Figures 4*a* and 4*b* show the integrated intensity maps of the main component of the (1, 1) and (2, 2) transitions, respectively, while Figure 4*c* shows the sum of the integrated emission of the main component of the (1, 1) and (2, 2) lines. The ammonia clumps Cep A-1, Cep A-2, and Cep A-3 are labeled in these figures. The position of the 14 radio continuum sources HW (Hughes & Wouterloot 1984) are indicated in these figures by crosses.

There are several important observational characteristics which can be noted from the integrated emission maps shown in Figure 4: (1) The stellar activity center is embedded in a small ($\leq 5''$) high-density clump. This activity center is $\sim 10''$ shifted northwest with respect to the axis of the Cep A-1 + Cep

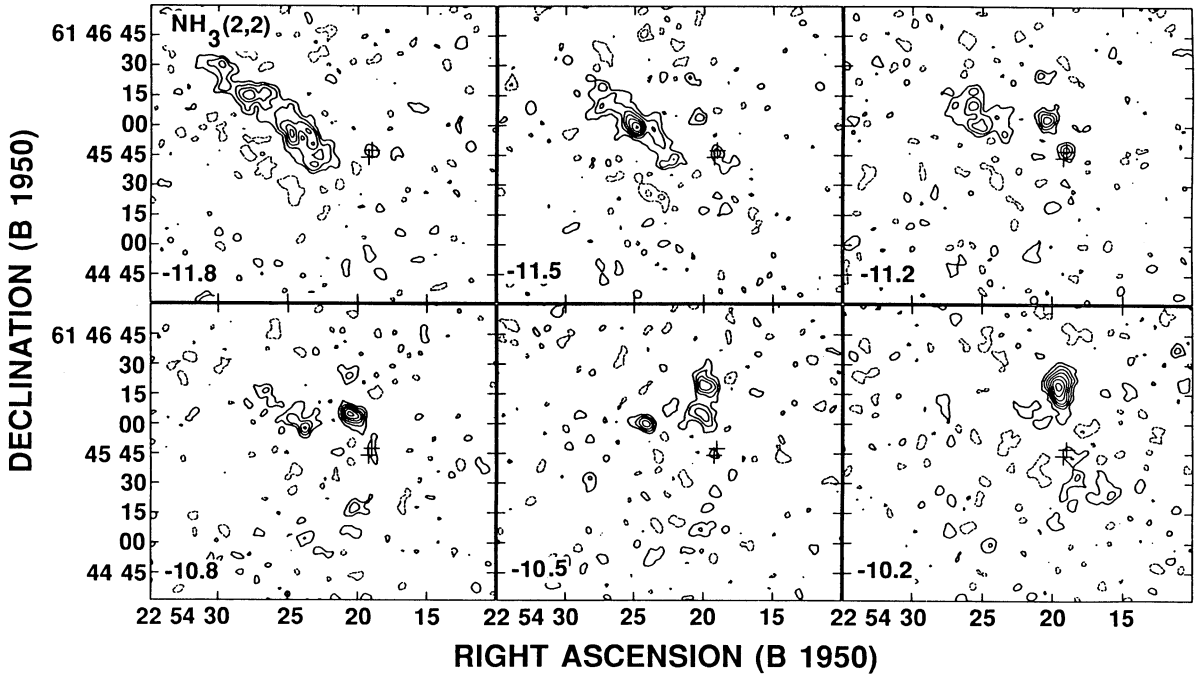

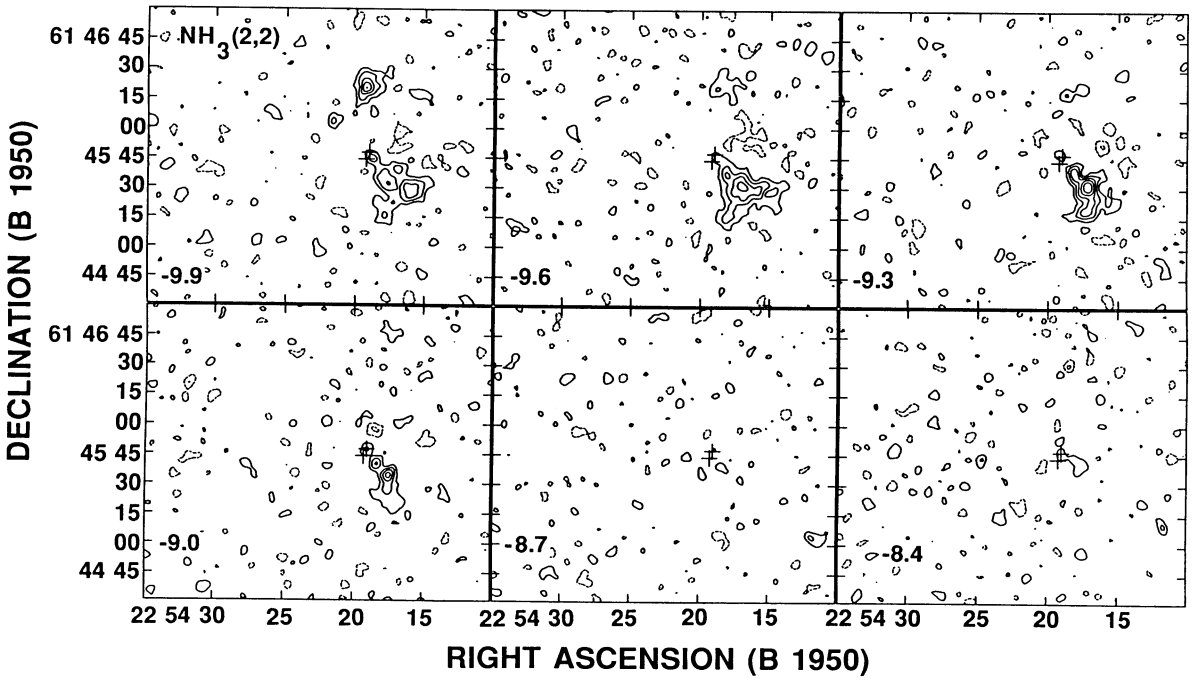

FIG. 1*b*

TABLE 1

FLUXES

Position[a]		$S_\nu(1, 1; m)$[b]	$S_\nu(1, 1; is)$[b]	$S_\nu(2, 2; m)$[b]		$T_R(22–11)$[d]
$\alpha(1950)$	$\delta(1950)$	(mJy beam^{-1})	(mJy beam^{-1})	(mJy beam^{-1})	$\tau(1, 1; m)$[c]	(K)
$22^h54^m17^s.27$	61°45′32″.0.....	126	55	96	1.5	23
22 54 19.38	61 46 19.0.....	156	73	113	1.7	22
22 54 20.23	61 46 05.0.....	137	58	92	1.3	22
22 54 24.60	61 46 01.0.....	119	47	79	1.1	22
22 54 25.72	61 46 07.0.....	111	41	56	0.8	19
22 54 27.56	61 46 13.0.....	133	50	76	0.9	20

[a] Positions of the observed peaks in the integrated intensity map of the (1, 1) transition (Fig. 4a).

[b] Peak fluxes observed at the selected positions. *m* and *is* refer to the main and inner hyperfine satellite lines, respectively. Synthesized beam $\simeq 5''$.

[c] Optical depth obtained from the $S_\nu(1, 1; m)/S_\nu(1, 1; is)$ ratio (Ho & Townes 1983).

[d] Rotational temperature obtained from the $S_\nu(2, 2; m)/S_\nu(1, 1; m)$ ratio (Ho & Townes 1983).

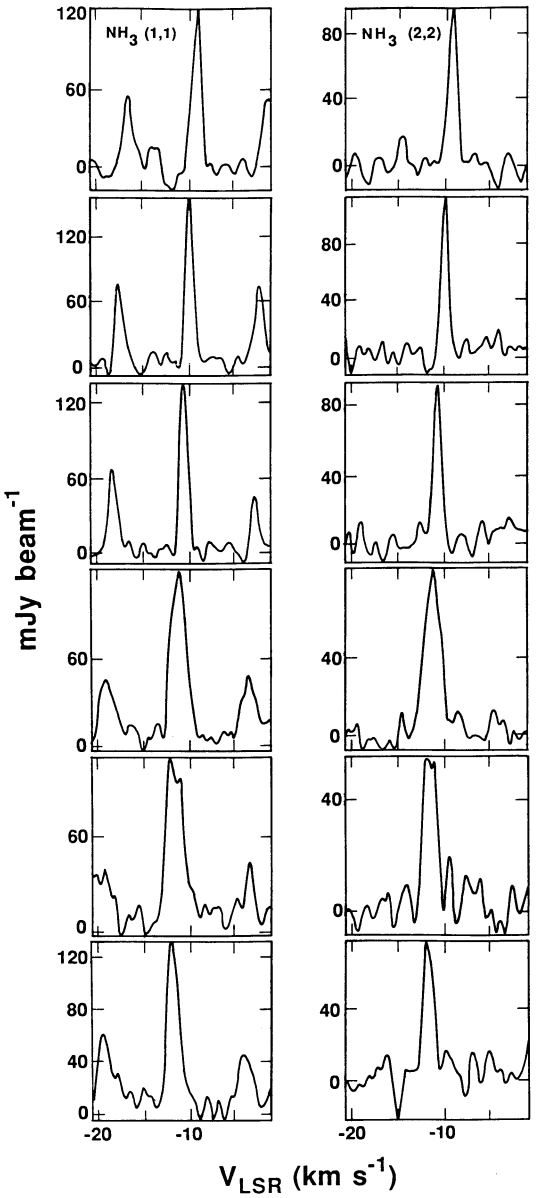

FIG. 2.—$NH_3(1, 1)$ (*left panels*) and $NH_3(2, 2)$ (*right panels*) spectra observed toward the positions indicated in Table 1. Each one of the panels from up to bottom of this figure corresponds to one of the six positions indicated in Table 1 in order of right ascension. Synthesized beam = 5″.4 × 5″.3 (p.a. = −54°).

A-3 interstellar disklike structure. (2) There is ammonia emission connecting Cep A-1 and Cep A-3 with the stellar activity center. In particular, note the bridge of the molecular gas from Cep A-3 to the activity center (see Fig. 4*c*). In contrast, there is no ammonia emission connecting Cep A-2 with the stellar activity center. (3) Most of the HW radio continuum sources follow the edges of the NH_3 condensations. This fact is more clearly observed in our present data than in THRC85 and THRC86. In particular, the location of sources HW 4, 5, and 6 at the border of the southern condensation of Cep A-2 was not evident in our previous data. (4) The ammonia emission in Cep

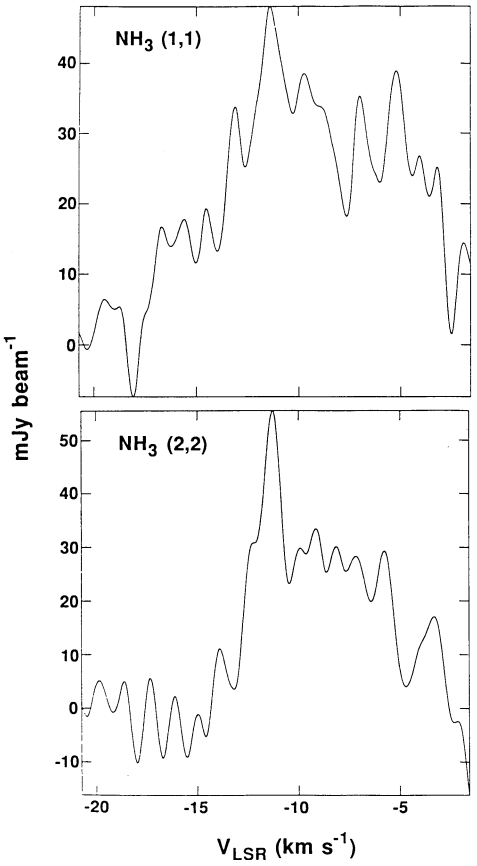

FIG. 3.—$NH_3(1, 1)$ and $NH_3(2, 2)$ spectra observed toward the position of HW 2, $\alpha(1950) = 22^h54^m19^s.0$, $\delta(1950) = 61°45'47''.3$ (Hughes & Wouterloot 1984). Synthesized beam = 5″.4 × 5″.3 (p.a. = −54°).

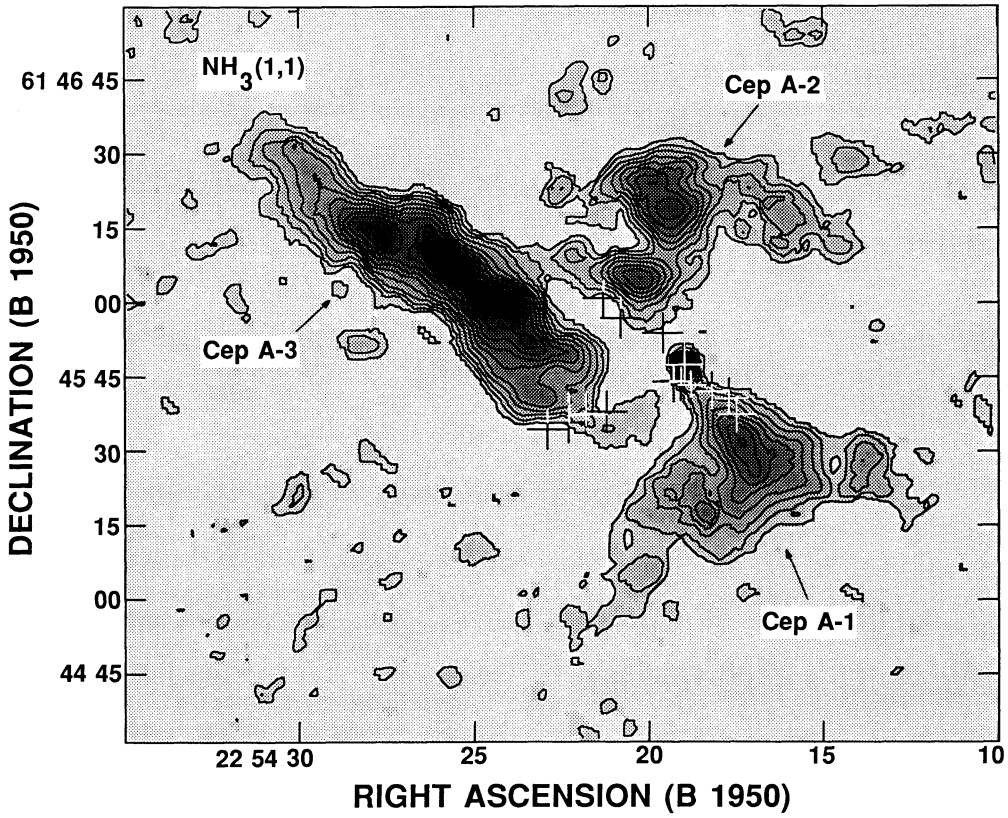

FIG. 4*a*

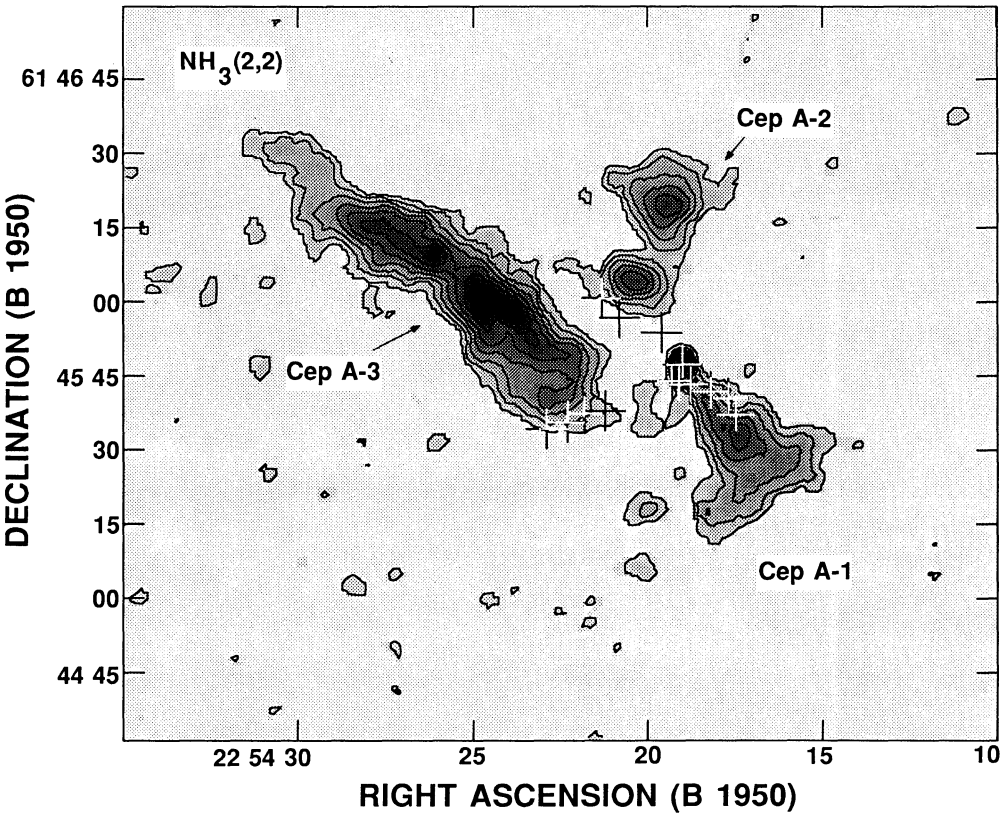

FIG. 4*b*

FIG. 4.—Contour and gray-scale maps of the integrated intensity of the (1, 1) (*a*), (2, 2) (*b*), and (1, 1) + (2, 2) (*c*) ammonia main hyperfine component. Contours are 1, 3, 5, 7, 9, 11, 13, 15, 17, 19, 21, 23, 25 times 10 mJy km s^{-1} $beam^{-1}$ (*a*), 1, 3, 5, 7, 9, 11, 13, 15 times 10 mJy km s^{-1} $beam^{-1}$ (*b*), and 1, 3, 5, 10, 15, 20, 25, 30, 35 times 10 mJy km s^{-1} $beam^{-1}$ (*c*). Synthesized beam = 5.″4 × 5.″3 (p.a. = −54°). Crosses indicate the positions of the 14 HW radio continuum sources (Hughes & Wouterloot 1984).

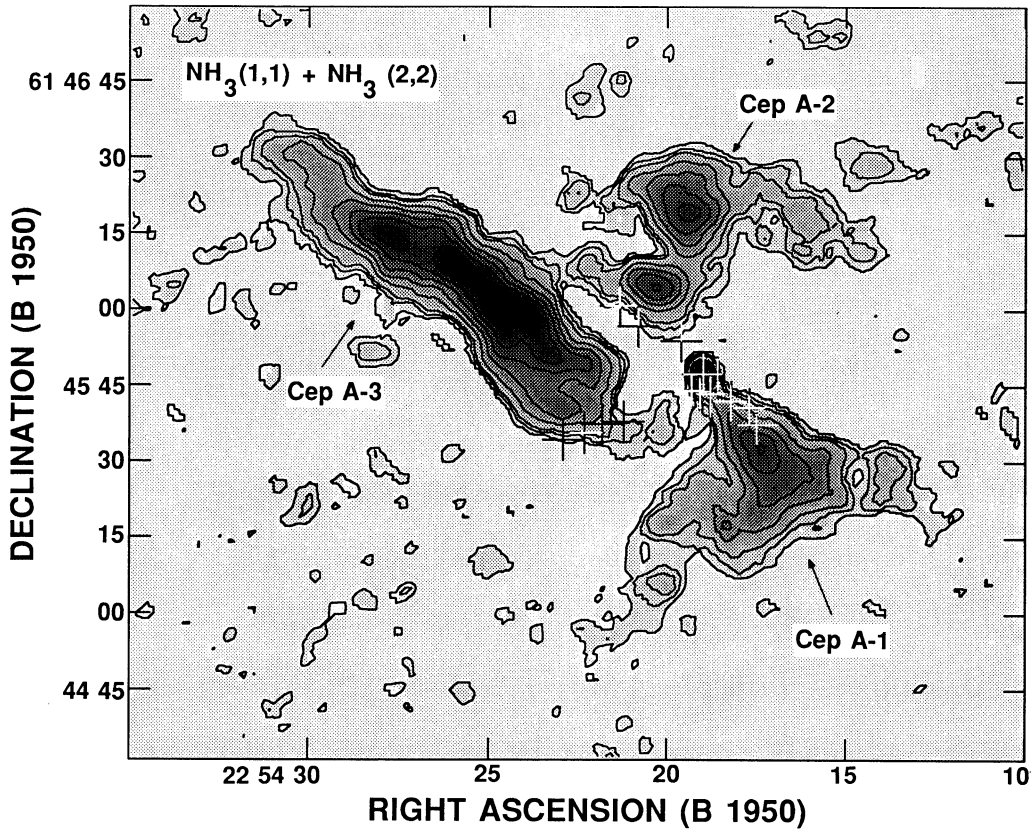

FIG. 4c

A-3 presents spatial undulations, while Cep A-1 and Cep A-2 show several arclike features at their edges (see Fig. 4c). We shall discuss all these four observational aspects in § 4.1.

From the ratio of the inner satellite hyperfines to the main line of the (1, 1) transition we have estimated the opacities $\tau(1, 1; m)$ at the peaks of the integrated intensity. We find that typical values for the opacities across the region are $\tau(1, 1; m) \simeq 2 \pm 1$ (see Table 1). From the $S_\nu(2, 2; m)/S_\nu(1, 1; m)$ ratio we have also estimated the rotational temperatures (see Ho & Townes 1983) toward those positions. Typical values $T_R(22\text{–}11) \simeq 20$ K are found (see Table 1). The principal parameters of the ammonia condensations are given in Table 2. These parameters have been obtained following the procedures explained in the footnotes of this table.

The total integrated flux in the (1, 1; m) line of the VLA ammonia condensations is ~ 15 Jy km s^{-1}, with most of the flux coming from Cep A-3 (~ 9 Jy km s^{-1}). This is $\sim 50\%$ of the flux seen with single-dish observations, ~ 30 Jy km s^{-1}, as we estimate from the data of Ho et al. (1982) and Güsten et al. (1984). If the remaining 50% of the single-dish flux is distributed smoothly within the VLA primary beam, it would contribute ~ 4 mJy beam^{-1} per channel, well below our 1 σ sensitivity level of 10 mJy.

3.2. *Gas Temperature Gradients*

In our previous observations (THRC86) we obtained with $\sim 10''$ of resolution an estimate of the gas temperature distribution by comparing the (2, 2) and (1, 1) ammonia emission. We found significant gas heating toward the stellar activity center. Based on these results, and the location of most of the HW radio continuum sources at the border of the ammonia condensations, we concluded that the edges of these condensations are being ionized and heated externally. We proposed that one or two central B1 stars, coinciding in position with the OH and H_2O masers in the region, are exciting most of the HW sources. With our present data of higher sensitivity and

TABLE 2

CONDENSATION PARAMETERS

Parameter	Cep A-1	Cep A-2	Cep A-3
Angular size $[l_a \times l_b]$[a]	0.8 × 0.6	0.7 × 0.5	1.6 × 0.4
Physical size $[l_a(\text{pc}) \times l_b(\text{pc})]$[a]	0.17 × 0.13	0.15 × 0.11	0.34 × 0.08
$\tau(1, 1; m)$	1.5	1.5	1.0
$\int S_\nu(1, 1; m)dV$ (Jy km s^{-1})[b]	2.8	2.6	9.3
$\int T_B(1, 1; m)dV$ (K km s^{-1})[c]	3.5	4.5	8.7
$T_R(22\text{–}11)$ (K)	23	22	20
$N(H_2)$ (10^{22} cm^{-2})[d]	6	8	12
$n(H_2)$ (10^5 cm^{-3})[e]	1.3	2.0	2.4
M ($M_\odot$)[f]	28	28	68

[a] Size of the emission at the 3 σ level.

[b] Integrated flux in the range $-13.2 \leq V_{LSR} \leq -8.5$ km s^{-1} over the surface indicated in note *a*. This flux has been corrected for the primary beam response.

[c] Integrated brightness temperature obtained from notes *a* and *b*.

[d] Average hydrogen column density over the surface indicated in note *a* and derived from $[N(H_2)/\text{cm}^{-2}] \simeq 8 \times 10^{21}\,[\tau/(1 - e^{-\tau})]\{[\int T_B(1, 1; m)dV]/(\text{K km s}^{-1})\}$, assuming $T_{ex} = T_R(22\text{–}11) = T_K$, and $X_{NH_3} = [NH_3/H_2] = 10^{-8}$ (Herbst & Klemperer 1973).

[e] Average hydrogen volume density derived from $n(H_2) = N(H_2)/l$, where $l = (l_a l_b)^{1/2}$.

[f] Mass estimated from $M = 2.64m(H)N(H_2) \times l_a \times l_b$ (considering elements heavier than H_2, He/H = 8%).

1993ApJ...410..202T

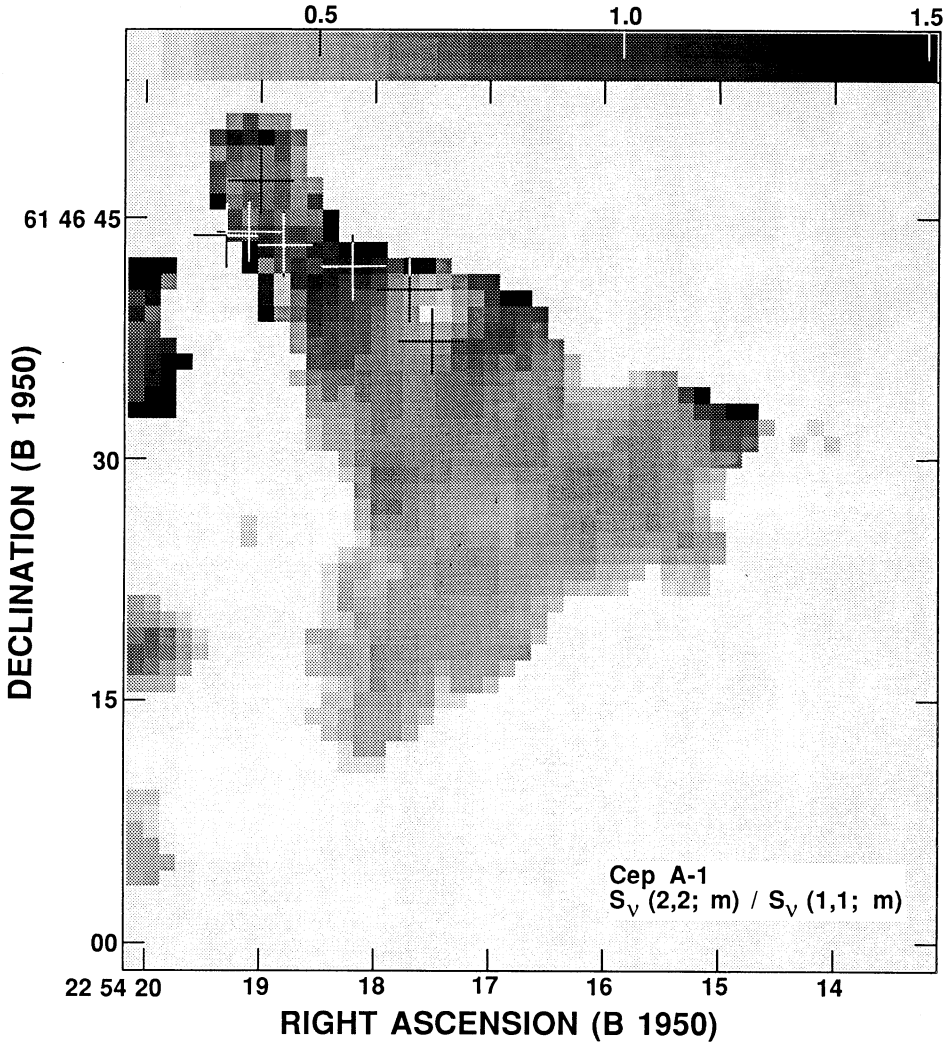

FIG. 5a

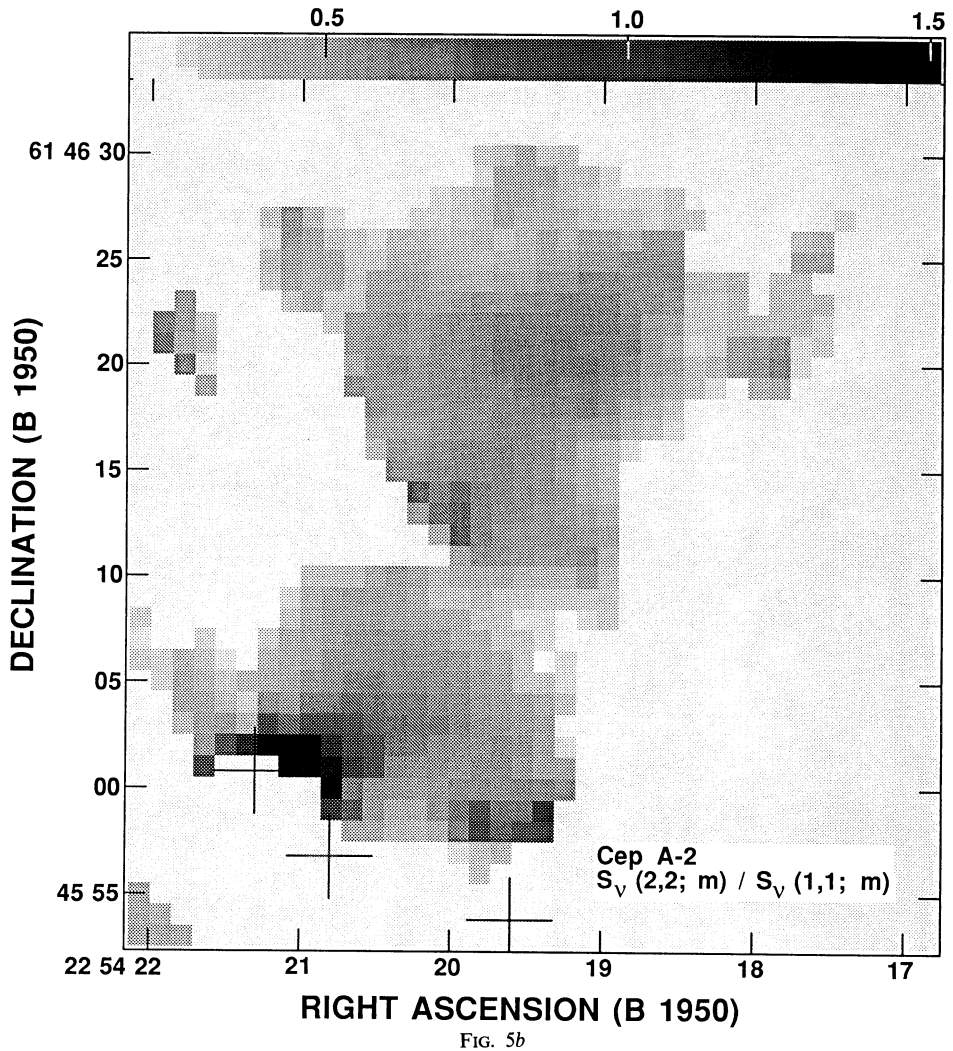

FIG. 5b

FIG. 5.—Gray-scale maps of the $S_\nu(2, 2; m)/S_\nu(1, 1; m)$ ratio in Cep A-1 (*a*), Cep A-2 (*b*), and Cep A-3 (*c*). Crosses indicate the position of the HW sources. Synthesized beam = 5″.4 × 5″.3 (p.a. = −54°).

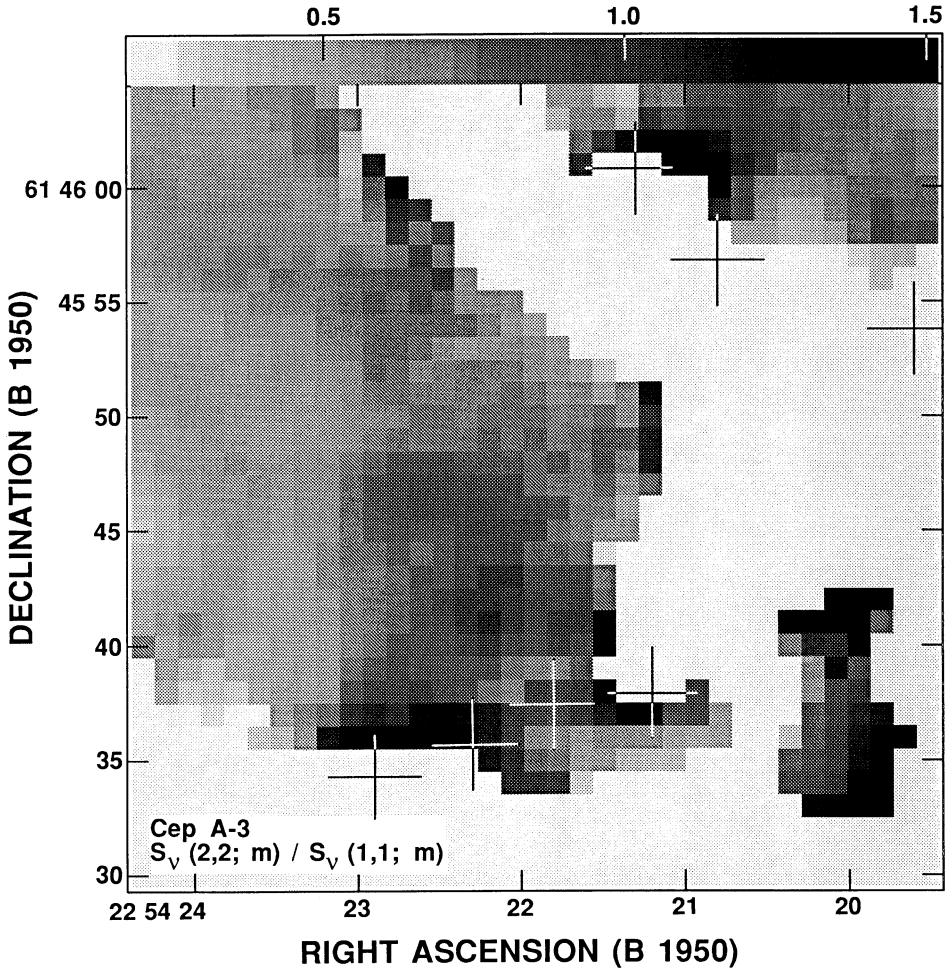

FIG. 5c

resolution we can now make a more detailed study of the heating of the molecular gas.

Figures 5*a*, 5*b*, and 5*c* show gray-scale maps of the (2, 2; *m*) to (1, 1; *m*) ratio in the Cep A-1, Cep A-2, and Cep A-3 ammonia condensations, respectively. To produce these maps we clipped the individual maps of the integrated intensity of the (2, 2) and (1, 1) ammonia main component at a level of 7 mJy beam^{-1} km s^{-1}. In this figure, the maps are presented separately in Figure 5 to make clearer the changes of the (2, 2; *m*) to (1, 1; *m*) ratio across the ammonia condensations. From these maps we see that the highest values of the (2, 2; *m*) to (1, 1; *m*) ratio are reached at the edges of the condensations, which face the stellar activity center. We note that this is not an artifact produced at the border of the condensations, because we have a high enough signal-to-noise ratio in these regions, and also because the (2, 2; *m*)/(1, 1; *m*) ratio at the edges of the condensations far away from the stellar activity center does not show such high values. From the (2, 2; *m*)/(1, 1; *m*) ratio, and adopting constant opacities $\tau(1, 1; m) = 1.5$ for Cep A-1 and Cep A-2, and $\tau(1, 1; m) = 1.0$ for Cep A-3 (see Table 2), we estimate that the rotational temperature gradients cover the ranges $15 \lesssim T_R(22\text{–}11) \lesssim 50$ K (Cep A-1), and $15 \lesssim T_R(22\text{–}11) \lesssim 30$ K (Cep A-2 and Cep A-3), with the highest temperatures toward the stellar activity center. From the peak of the (1, 1) and (2, 2) fluxes measured toward HW 2 (Fig. 3) we estimate, assuming an opacity of $\tau(1, 1; m) \simeq 1$, a rotational temperature $T_R(22\text{–}11) \simeq 40\text{–}50$ K at this position. Allowing for the rapid downward decays within each K-ladder, $T_R(22\text{–}11)$ can be used to estimate the kinetic gas temperature T_K (Walmsley & Ungerechts 1983; Danby et al. 1988). We therefore derive $T_K \gtrsim 40$ K for values $T_R(22\text{–}11) \simeq 30$ K, and $T_K \gtrsim 100$ K for values $T_R(22\text{–}11) \simeq 50$ K.

Moriarty-Schieven et al. (1991) have observed with 16″ resolution the inner region of the Cepheus A core in the CS(J = 7–6) line, which is sensitive to warm ($T_K > 30$ K) high-density [$n(H_2) > 10^5$ cm^{-3}] gas. Interestingly, their CS(J = 7–6) map shows two peaks of emission. The weaker peak coincides with HW 2, where we observe a significant heating in NH_3. The stronger peak is 20″ southeast of HW 2, coinciding with the SW end of Cep A-3, in agreement with the fact that Cep A-3 is the stronger condensation observed in NH_3, with high rotational temperatures at the edges which face the stellar activity center.

We shall discuss in § 4.2 the theoretical implications of these observed gas temperature gradients.

3.3. *Kinematics of the Region*

In order to study the velocity field of the ammonia emission in the region we have made first-order moments of the (1, 1; *m*) and (2, 2; *m*) lines. Their gray-scale maps are shown in Figures 6*a* and 6*b*. It is apparent from these figures that the mean velocity of the emission in Cep A-1, Cep A-2, and Cep A-3 are

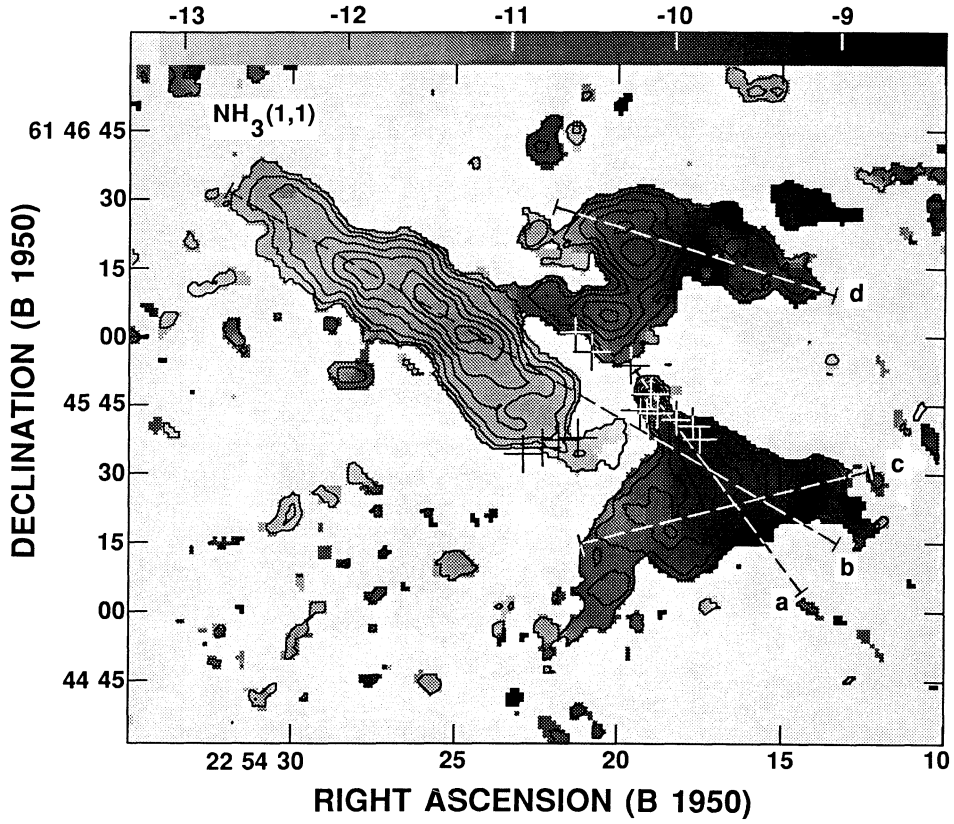

FIG. 6*a*

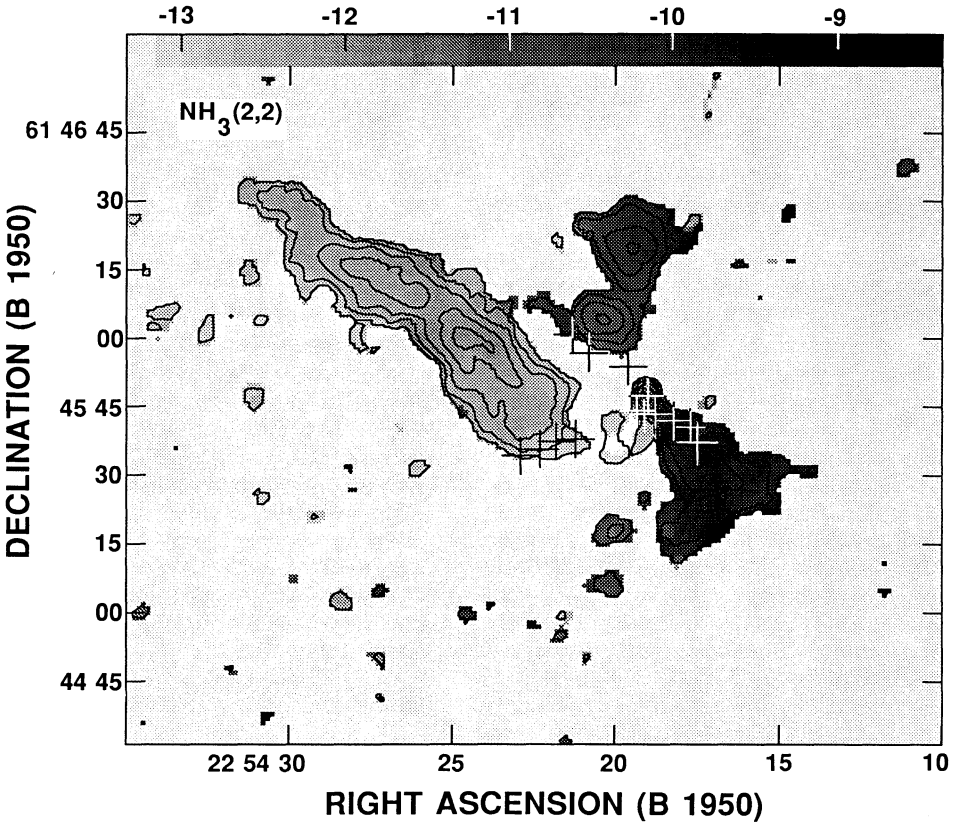

FIG. 6*b*

FIG. 6.—Gray-scale maps of the first-order moment (mean velocity) of the (1, 1) (*a*) and (2, 2) (*b*) ammonia main component line superposed on the contour maps of the integrated intensity of the (1, 1) (*a*) and (2, 2) (*b*) main component. Gray scales range from -13.3 to -8.4 km s^{-1}. Contours are 1, 3, 6, 10, 14, 18, 22 times 10 mJy km s^{-1} beam^{-1} (*a*), and 1, 3, 6, 10, 14 times 10 mJy km s^{-1} beam^{-1} (*b*). Crosses indicate the positions of the 14 HW sources. Dashed lines in (*a*) indicate the direction of the cuts of the position-velocity (moment 1) diagrams shown in Fig. 7.

$V_{LSR} \simeq -9.5$, -10.0, and -12.0 km s^{-1}, respectively. Within Cep A-1 and Cep A-2 there are internal velocity variations of ~ 1 and 2 km s^{-1}, respectively, with the lower velocities (~ -11.0 km s^{-1}) in the eastern parts of these condensations. Especially remarkable is the abrupt change of velocity from -9.5 to -11.0 km s^{-1} in the southeastern edge of the Cep A-1 condensation (see Fig. 6*a*). Cep A-3 presents an almost constant velocity of ~ -12 km s^{-1} along the structure. However, the gas connecting this structure with the stellar activity center is blueshifted ($V_{LSR} \simeq -13$ km s^{-1}) with respect to all the velocities observed in the ammonia emission. This is also seen in Figure 7, where we show several cuts of the first-order moment map of the (1, 1; *m*) transition along the directions indicated in Figure 6*a*.

As we noted in § 3.1, the ammonia clump associated with HW 2 has large line widths, $\Delta V \simeq 7$ km s^{-1}, as observed with 5″ resolution. In a very recent paper (Torrelles et al. 1993, hereafter TRCH93), we have studied this condensation with the highest angular resolution available with our present observations, 2.″4 × 2.″2 (uniform weighting). We found (TRCH93) that this clump has a deconvolved size of 3.″3 × 2.″3 (p.a. = 22°), or 2400 × 1700 AU, a density $n(H_2) \simeq 3 \times 10^7 (X_{NH_3}/10^{-8})^{-1}$ cm^{-3}, and a mass of $\sim 2(X_{NH_3}/10^{-8})^{-1}$ $M_\odot$, where $X_{NH_3} = (NH_3/H_2)$ is the abundance ratio. (Please note that in our earlier paper TRCH93, the explicit dependence on abundance was expressed as proportional rather than inversely proportional. All the numerical factors were correct, but all expressions X_{NH_3} should be $X_{NH_3}^{-1}$.) We also found velocity variations of ~ 4–5 km s^{-1} across this circumstellar structure, with a velocity gradient of ~ 300 km s^{-1} pc^{-1} along its major axis. These velocity variations and the broad ammonia line widths of 7 km s^{-1} observed toward HW 2 with 5″ resolution (this paper) seem to be produced by three overlapping velocity components at $V_{LSR} \simeq -12$, -9, -6 km s^{-1}, with individual line widths $\Delta V \simeq 2$ km s^{-1} (TRCH93). We also noted (TRCH93) that HW 2 is a double radio source at $\lambda = 2$ cm (Hughes 1988), separated by $\sim 0.''2$ (~ 150 AU) and oriented with p.a. = 30°–40°. On the basis of these results we suggested (TRCH93) that this clump could represent a circumstellar molecular disk associated with a massive young star, probably related to the circumstellar disk independently proposed from infrared and H_2O and OH maser observations (Lenzen et al. 1984, Joyce & Simon 1986; Lenzen 1988; Cohen et al. 1984). Within this scenario, the double radio source of HW 2 could represent the ionized inner part of the circumstellar disk, in the same way as proposed by Rodríguez et al. (1986) to explain the double radio continuum source in L1551. The velocity variations that we observe in the circumstellar high-density gas associated with HW 2 could be due to bound motions of the molecular gas (e.g., infall or rotation) close ($\lesssim 1500$ AU) to a central mass of $\lesssim 10$–20 $M_\odot$. This mass is on the order of the mass of the star(s) proposed in THRC85 and

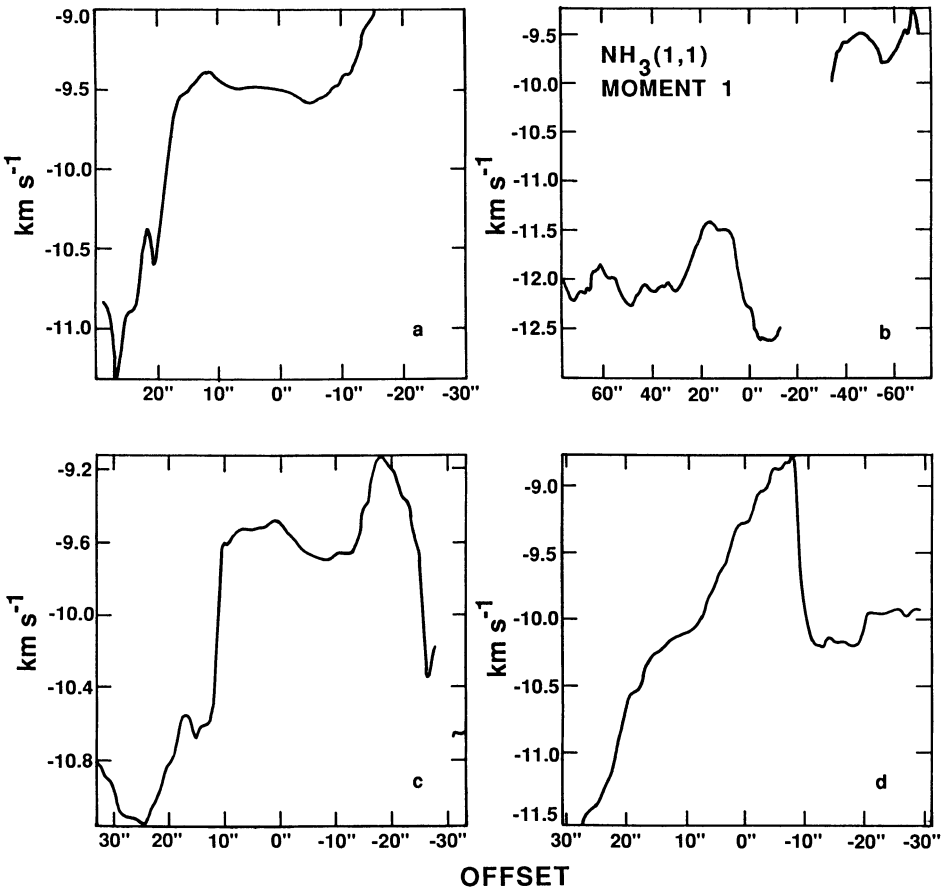

FIG. 7.—Different position-velocity (moment 1) diagrams of the NH_3 (1, 1) line along the directions indicated in Fig. 6*a* by dashed lines and numbered there with letters a, b, c, and d. Offset positions increasing in right ascension are with respect to $\alpha(1950) = 22^h54^m17^s.01$, $\delta(1950) = 61°45'27''.7$ (*a*), $\alpha(1950) = 22^h54^m22^s.74$, $\delta(1950) = 61°45'53''.5$ (*b*), $\alpha(1950) = 22^h54^m16^s.67$, $\delta(1950) = 61°45'22''.5$ (*c*), and $\alpha(1950) = 22^h54^m17^s.72$, $\delta(1950) = 61°46'17''.5$ (*d*).

THRC86 to account for the number of ionizing photons required to excite the H II bright rims of the region. However, we must note, as also noted in THRC93, that the kinematics of this circumstellar molecular structure could be strongly affected by the powerful wind of the central source, making it difficult to distinguish at these circumstellar scales between bound motions (e.g., infall or rotation) and expanding motions. Higher angular resolution and sensitivity observations are clearly needed in order to better resolve the ammonia emission associated with HW 2, and in this way, to present a more detailed model for the kinematics of this possible circumstellar ($\sim 10^3$ AU) molecular disk.

4. DISCUSSION

4.1. *Analysis of the Rotating Interstellar Disk Scenario: Reorientation of the Molecular Outflow?*

In THRC85 and THRC86, we suggested that the high-density condensations Cep A-1, Cep A-2, and Cep A-3 may play an important role in focusing the bipolar outflow observed by Rodríguez et al. (1980). In particular, in THRC86 we proposed that Cep A-1 and Cep A-3 constitute a single interstellar disklike structure with a rotation curve flat to within 15″ of the stellar activity center. The location of the powering source(s) of the outflow at the northwest edge of the interstellar disklike structure led us to propose that the outflow escapes more easily in the northwest direction but is trapped in the southeast direction by the higher pressure of the ammonia disk, explaining in this way why the redshifted CO lobe observed by Rodríguez et al. (1980) is more extended than the blueshifted one. However, because of the relatively low angular resolution of the CO observations ($\sim 1'$), it was not possible at that time to know if the blue- and redshifted CO lobes have similar morphologies close to the activity center, and therefore to know more precisely the role of the interstellar disklike structure in the collimation of the outflow at smaller scales. With the present ammonia results and the 15″ resolution CO observations of Bally & Lane (1991, 1992) we are able now to make a more detailed comparison.

Figure 8 shows a superposition of the high-velocity CO emission (Bally & Lane 1991, 1992) and the sum of the integrated intensity of the (1, 1; *m*) and (2, 2; *m*) lines (from Fig. 4*c*). It is apparent from this figure that the CO outflow, in the inner region, presents a rather complicated quadrupolar morphology, with an overall east-west orientation. This orientation is clearly not perpendicular to the interstellar disklike ammonia structure constituted by Cep A-1 and Cep A-3, oriented in the northeast-southwest direction. The most noticeable of this superposition is that Cep A-1 is located in the midst of the two main western redshifted CO lobes, while Cep A-3 is in between the two eastern blueshifted ones. It follows from this result that the high-density interstellar disklike structure cannot provide the focusing mechanism of the outflow in the east-west direction, at least in terms of the scenario proposed by Barral & Cantó (1981) and Torrelles et al. (1983) of an interstellar disk or toroid collimating the molecular outflow along the poles of such a structure.

The morphology of the Cep A-east CO outflow observed by Bally & Lane (1991, 1992), with multiple lobes, is quite similar to that observed in L723 by Avery, Hayashi, & White (1990). Both outflows show multiple CO lobes with an overall quadrupolar morphology. For L723, Avery et al. (1990) suggested that the quadrupolar lobes are tracing the walls of evacuated cavities swept clear by a wind. We have considered the possibility that this scenario is working in Cepheus A. We believe, however, that this is not the case. As mentioned above, the Cep A-1 + Cep A-3 disklike structure is situated between the CO lobes (see Fig. 8). This result indicates that the areas between the two pairs of blue- and redshifted lobes are occupied by high-density gas, with no evidence of cavities there. We think that the location of the high-density gas in between the CO lobes is not a projection effect, but that they are spatially associated because we find heating of the gas and broadening of the ammonia lines toward the position of the proposed powering source of the molecular outflow, HW 2 (see §§ 3.1, 3.2, and 3.3).

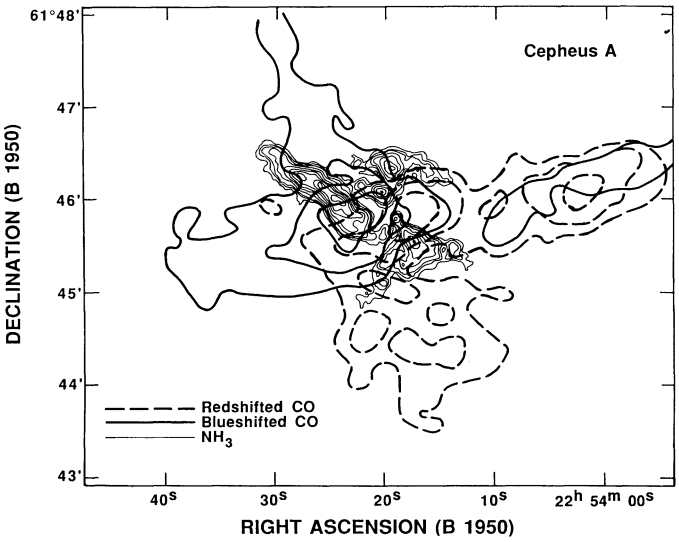

FIG. 8.—Superposition of the high-velocity CO emission of the inner region of Cepheus A (Bally & Lane 1991, 1992) and the sum of the integrated intensity of (1, 1; *m*) and (2, 2; *m*) lines (from Fig. 4*c*).

On the basis of the spatial disposition of the high-density gas with respect to the molecular outflow and their physical association, we propose the following scenario in order to explain the morphology of the CO outflow in Cepheus A-east: The exciting star(s) related to HW 2, located at the northwest edge of the interstellar disklike ammonia structure, has an associated wind which is mostly collimated in the east-west direction at circumstellar scales (Cohen et al. 1984) and which is related to the circumstellar molecular structure discussed in § 3.3 (see also TRCH93). This wind is producing a molecular outflow which could be interacting with the high-density gas traced by the ammonia emission. In this interaction, the blue- and redshifted east-west lobes of the bipolar outflow are split in two halves by Cep A-1 and Cep A-3, respectively, producing the overall quadrupolar structure of the molecular outflow. Therefore, within this scenario, the high-density gas would *divert* and *redirect* the molecular outflow at scales of $\gtrsim 0.05$ pc, the projected distance from the stellar activity center to the axis of symmetry of the Cep A-1 + Cep A-3 disklike structure.

Such a proposed interaction should manifest itself in a perturbation of the high-density gas, and in fact we think that there are some observational indications in terms of morphological and kinematical effects on the ammonia gas which support this thesis.

As mentioned in § 3.1, the emission in Cep A-3 presents spatial undulations. We believe that these corrugations could

be due to hydrodynamical instabilities of Kelvin-Helmholtz type produced as a consequence of the interaction of the molecular outflow with the surface of Cep A-3, as a result of the different densities in two fluids in relative motions.

Lamb (1932) considered the case of two incompressible fluids with densities n_1 and n_2, one beneath the other, moving parallel with relative velocity V. He showed that small perturbations in the common surface of the two fluids with gravity g can be characterized by oscillations of wavelengths λ about a state of steady motion, with the condition for instability of the common surface of the interaction given by (see also Shu 1992)

$$V^2 \geq V_c^2 = g\left(\frac{2\pi}{\lambda}\right)^{-1} \frac{n_1^2 - n_2^2}{n_1 n_2}, \quad (1)$$

and the growing time for these oscillations given by

$$\tau = \left(\frac{2\pi}{\lambda}\right)^{-1} \frac{(n_1 + n_2)}{V\sqrt{n_1 n_2}} \left(1 - \frac{V_c^2}{V^2}\right)^{-1/2}. \quad (2)$$

If we assume that the overall interaction of the molecular outflow with Cep A-3 can be dealt with an interaction of two incompressible fluids, then we can apply the analysis developed by Lamb (1932). Assuming a flattened mass distribution in Cep A-3, the gravity at the surface of the interaction is given by $g \simeq GM_c/l^2$, with M_c the mass of Cep A-3 ($\sim 68\ M_\odot$, Table 2) and $2l$ the size of Cep A-3 (~ 0.34 pc, Table 2). Taking $n_1 \simeq 10^5$ cm^{-3}, the estimated hydrogen volume density for Cep A-3 (Table 2), $n_2 \simeq 10^3$ cm^{-3}, a reasonable density for the molecular outflow, $V \simeq 10$ km s^{-1}, the velocity of the molecular outflow relative to Cep A-3 (Hayashi, Hasegawa, & Kaifu 1988), and $\lambda = 0.08$ pc, a characteristic scale for the oscillations estimated from Figure 4*c*, we can see that equation (1) is verified with $V \simeq 10$ km s$^{-1} > V_c \simeq 6$ km s^{-1}. Furthermore, we obtain from equation (2) $\tau \simeq 2 \times 10^4$ yr, which is of the order of the dynamical time of the molecular outflow (Hayashi et al. 1988). It follows from this that it is plausible that these Kelvin-Helmholtz instabilities have grown at the surface of Cep A-3 during the outflow time.

We also believe that the filamentary structures observed at the edges of Cep A-1 and Cep A-2 could have been created by pushing and dragging of this high-density gas by the outflow. This could explain the blueshifted component of the eastern edge of Cep A-1, in the direction of the blueshifted molecular outflow, as well as the east-west velocity gradient observed in Cep A-2, with the highest velocities to the west, in the direction of the redshifted molecular outflow (see Figs. 6 and 8).

Hayashi et al. (1988) suggested that the ammonia condensations Cep A-1, Cep A-2, and Cep A-3, as a whole, are part of a low-velocity outflow of dense gas. If this is the case, the momentum contained in the high-velocity CO outflow would be much lower ($\sim 20\ M_\odot$ km s^{-1}; Hayashi et al. 1988) than the momentum in the outflow of dense gas ($\sim 200\ M_\odot$ km s^{-1}; this paper). An alternative possibility is that the overall observed motions in the interstellar high-density gas represent bound motions rather than part of an outflow, given that the estimated mass in the high-density molecular gas, $\sim 120\ M_\odot$ (Table 2), and the mass provided by the central star(s), ~ 10–$20\ M_\odot$ (THRC85; THRC86; this paper), seem to be enough to bind them. However, as mentioned above, we think it is quite plausible that part of the high-density gas located at the edges of the ammonia clumps is being incorporated, by a dragging effect, into the general molecular outflow.

We would like to point out here that the proposed scenario to explain the quadrupolar morphology of the molecular outflow far away from the activity center (≥ 0.05 pc) is independent of whether or not Cep A-1 + Cep A-3 constitute an interstellar disk.

Are Cep A-1 and Cep A-3 part of an interstellar disk? We think that there are several observational indications favoring this. Cep A-1 + Cep A-3 constitutes a very elongated structure ($\sim 0.5 \times 0.08$ pc), with a velocity field consistent with flat rotation motions bound by the internal mass (THRC86; this paper). Furthermore, the orientation of this elongated structure, coinciding with the orientation of the Galactic plane, is very similar to that presented in the ^{13}CO and ^{12}CO ambient emission at much larger scales (~ 6 pc; Sargent 1977), as well as in NH_3 observed with single-dish (~ 1 pc; Ho et al. 1982; Güsten et al. 1984). Since the molecular outflow is observed only at scales of $\lesssim 0.5$ pc, and it is much less massive ($\sim 10\ M_\odot$; Hayashi et al. 1988) than the ^{13}CO and NH_3 structures ($\gtrsim 100\ M_\odot$), it is hard to imagine that the outflow can produce such a large elongation in the disklike structure. In fact, if the elongation has been produced from a spherical high-density core by the action of a bipolar outflow, sweeping clear the high-density gas along the direction of the outflow, one would expect then to observe an amount of mass in the molecular outflow comparable with the mass of the elongated core. But this is not the case. We then think that it is more reasonable that the observed elongation in the ambient molecular structures in Cepheus A preceded rather than followed the star formation in the region (see also other regions, Rodríguez 1989; Myers et al. 1991; Torrelles et al. 1992; Estalella et al. 1992), probably favored by the alignment with the Galactic plane.

Within the interstellar disk scenario, we should expect to find the activity center of the star formation at the axis of symmetry of such a disk. We find that the powering source related to HW 2 is displaced to the northwest of the elongated interstellar ammonia structure. However, we think that it is possible that the exciting star has moved from its original position. In fact, assuming that it has been formed originally at the axis of symmetry of the interstellar disk ammonia structure, but that it has acquired proper motions of ~ 1 km s^{-1} with respect to the ambient gas (a typical velocity for turbulent motions), it would need $\sim 4 \times 10^4$ yr to reach its present position. This time is similar to the dynamical time of the molecular outflow (Hayashi et al. 1988). It follows from this that the central star has had enough time to move to its current position. The observed link of high-density gas between Cep A-1 and Cep A-3 and the stellar activity center (see Fig. 4*c*) is also indicative of a relationship between the interstellar disklike structure and the young massive star(s). Furthermore, it is plausible that the gas connecting Cep A-3 with Cep A-1 and the stellar activity center is even hotter than that reported here. Observations of higher transitions of ammonia—for example, $NH_3(3, 3)$—probably would help to observe more clearly such a hot molecular gas.

In any case, if Cep A-1 and Cep A-3 indeed constitute an interstellar disk, it seems clear from our observations that the wind(s) and ionizing flux associated with the central young star(s) are starting to disrupt it.

4.2. *On the Origin of the Gas Temperature Gradients*

In § 3.2 we have shown that there are rotational temperature $T_R(22\text{–}11)$ gradients in the ammonia gas, with the highest tem-

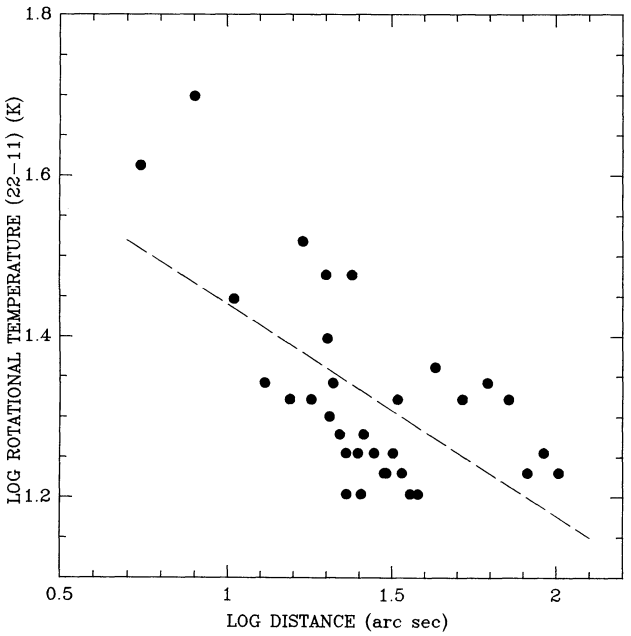

FIG. 9.—Rotational temperature between the (2, 2) and (1, 1) ammonia transitions as a function of the angular distance to the source HW2, $\alpha(1950) = 22^h54^m19^s.0$, $\delta(1950) = 61°45'47''.3$. Dashed line indicates the least-square fit to the data, $[T_R(22\text{–}11)/\mathrm{K}] = 51[r/3.5 \times 10^{-3}\ \mathrm{pc}]^{-0.3}$ (see § 4.2).

peratures toward the stellar activity center, at the edges of the ammonia clumps. The rotational temperatures we derive toward HW 2, $T_R(22\text{–}11) \simeq 40\text{–}50$ K, are consistent with that obtained in our previous work (THRC86).

We have calculated the projected offset positions r with respect to HW 2 along cuts of the $S_\nu(2, 2; m)/S_\nu(1, 1; m)$ maps shown in Figure 5, by steps of 5″, and fitted their temperatures by the expression $T_R(22\text{–}11) \propto r^{-\alpha}$. For the individual cuts of temperature along the major axis of the Cep A-1, Cep A-2, and Cep A-3 condensations, we obtain, respectively, indices $\alpha = 0.6$, 0.6, and 0.3. Fitting a single power-law relation to all the values obtained along the individual ammonia condensations, we obtain a relation given by (see Fig. 9)

$$\left[\frac{T_R(22\text{–}11)}{\mathrm{K}}\right] = 51\left(\frac{r}{3.5 \times 10^{-3}\ \mathrm{pc}}\right)^{-0.3}. \quad (3)$$

These indices are very similar to those expected if the ammonia gas is heated via collisions with hot dust, which in turn is heated by the absorption of the radiation emitted by a central star(s). In fact, Scoville & Kwan (1976), and Loren & Wootten (1978) have estimated that the dust temperature at a distance r of a star with luminosity L_* is given by

$$\left(\frac{T_d}{\mathrm{K}}\right) \simeq 23\left(\frac{L_*}{10^{38}\ \mathrm{ergs\ s^{-1}}}\right)^{0.2}\left(\frac{r}{\mathrm{pc}}\right)^{-0.4}, \quad (4)$$

therefore with an index $\alpha = 0.4$ very similar to those we obtain for the ammonia gas temperatures. From infrared measurements the luminosity of the central star(s) is estimated to be $L_* \simeq 2.5 \times 10^4\ L_\odot$ (Evans et al. 1981; Lenzen et al. 1984). Taking this luminosity, we estimate a dust temperature $T_d \simeq 90$ K at a distance $r = 0.03$ pc, which is the distance at which temperatures up to $T_R(22\text{–}11) \simeq 40\text{–}50$ K, or $T_K \sim 100$ K (Walmsley & Ungerechts 1983; Danby et al. 1988), is observed. Since collisional coupling of the gas and dust is expected for densities $n(\mathrm{H_2}) \gtrsim 10^5\ \mathrm{cm^{-3}}$ (Goldsmith & Langer 1978), a value which is consistent with the density derived in this paper for the ammonia condensations (see Table 2), we think that the main heating of the ammonia gas in Cepheus A is via collisions with hot dust, heated by the luminosity of the central star(s).

Ammonia studies made in other star-forming regions also suggest the presence of gradients in rotational temperature. Combining single-dish and VLA data, Garay & Rodríguez (1990) detected gradients in density and rotational temperature in G34.3+0.2. Keto, Ho, & Haschick (1987), and more recently Garay, Moran, & Rodríguez (1992) reported evidence for a gradient in the ammonia rotational temperature in G10.6−0.4 and G10.47+0.03, respectively. Table 3 summarizes the rotational temperature gradients found toward these sources as well as toward Cepheus A. In this table, column (1) gives the name of the source, column (2) gives the index of the power-law fit, column (3) gives the rotational temperature at a distance of 0.1 pc, column (4) gives the luminosity associated with the exciting star(s), and column (5) gives the references. It is evident from the results of Table 3, that the larger the luminosity of the exciting star(s), the larger the rotational temperature at 0.1 pc. This correlation suggests that the determination of ammonia rotational temperatures as a function of distance from the star could, after calibration of the method is achieved, provide a means of estimating the luminosity of the exciting star or stars in the region.

Finally, we would like to point out here that this analysis of temperature distribution stresses the powerful capability of the VLA system and opens the possibility to making further similar studies in other star-forming regions. This will certainly help toward achieving a better understanding of the interaction of young stars with the ambient molecular gas.

5. CONCLUSIONS

The $(J, K) = (1, 1)$ and (2, 2) NH_3 lines were mapped toward Cepheus A with $\sim 2''$ of angular resolution and ~ 0.3 km s^{-1} of

TABLE 3

SOURCES WITH REPORTED GRADIENTS IN AMMONIA ROTATIONAL TEMPERATURE

Source (1)	Index (α)[a] (2)	T_R (at 0.1 pc)[a] (3)	L_* ($L_\odot$) (4)	References (5)
G10.6−0.4	0.5	100	10^6	Keto et al. 1987
G34.3+0.2	0.6	83	3×10^5	Garay & Rodríguez 1990, Garay et al. 1986
G10.47+0.03	0.4	46	6×10^4[b]	Garay et al. 1992, Wood & Churchwell 1989
Cepheus A	0.3	20	3×10^4	This paper, Lenzen et al. 1984

[a] $T_R \propto r^{-\alpha}$ (see § 4.2).
[b] Assuming, from Wood & Churchwell 1989, that two B0 and one B0.5 ZAMS stars excite the region.

velocity resolution. We have reached a sensitivity of 10 mJy per channel. These observations have shown with detail the spatial and kinematics structure of the ambient high-density gas. The ammonia gas of Cep A-1 and Cep A-3 constitutes an interstellar ($\sim 2'.3 \times 0'.4$, or $\sim 0.5 \times 0.08$ pc) elongated structure, with the stellar activity center located at the northwest edge of this structure. Cep A-2 is constituted by two condensations. Cep A-1 and Cep A-3 are located, respectively, between the two main pairs of blue- and redshifted lobes of the molecular outflow. It follows from this that the interstellar disklike ammonia structure cannot collimate the originally east-west orientation of the bipolar outflow. We propose that the interstellar high-density gas is *diverting* and *redirecting* the outflow, in the sense that the quadrupolar structure of the molecular outflow is produced by the interaction with the ammonia condensations, with Cep A-1 and Cep A-3 splitting in two halves, respectively, the blue- and redshifted lobes of an east-west bipolar molecular outflow. This interaction seems to be producing a perturbation in the morphology and kinematics at the edges of the ammonia condensations. Some of the high-density gas at the edges of the condensations could be in the process of being incorporated into the general high-velocity molecular outflow by a dragging effect. However, we argue that the elongated interstellar high-density ammonia structure precedes rather than follows the outflow phase, and that the overall kinematics of this high-density gas can be explained by bound motions due to the molecular and stellar masses of the region.

HW 2 is embedded in a circumstellar ($3''.4 \times 2''.3$, or 2400×1700 AU) high-density [$n(H_2) \simeq 3 \times 10^7 (X_{NH_3}/10^{-8})^{-1}$ cm^{-3}] clump of mass $\sim 2(X_{NH_3}/10^{-8})^{-1} M_\odot$, with large velocity dispersions (~ 3–4 km s^{-1}) and high temperatures [$T_R(22\text{–}11) \simeq 40$–50 K]. This result gives further support to HW 2 as the exciting source of the outflow as well as of the bright radio rims which are found to be following the edges of the ammonia condensations (THRC85; THRC86; this paper). The motions of the ammonia gas close to HW 2 can be produced by bound motions of the gas (e.g., rotation or infall) around a central mass of ~ 10–$20\ M_\odot$, or alternatively by the wind of the central source.

We have analyzed the temperature gradients in the high-density molecular gas. The highest temperatures are found at the edges of the ammonia condensations which face the stellar activity center. We find that temperatures as a function of projected distance r with respect to HW 2 can be fitted by $T_R(22\text{–}11) \propto r^{-\alpha}$, with $\alpha = 0.3$–0.6. These indices are very similar to the index expected if the gas is heated via collisions with hot dust, which in turn is heated radiatively by the luminosity of the central star(s). The observed luminosity in the region ($\sim 2.5 \times 10^4\ L_\odot$) is high enough to heat the gas up to the observed values, $T_R(22\text{–}11) \simeq 40$–50 K, or $T_K \sim 100$ K. The analysis of molecular gas temperatures carried out with the VLA in Cepheus A opens the possibility to make similar studies in other star-forming regions.

Finally, if the condensations Cep A-1 and Cep A-3 indeed constitute an interstellar disk, it seems clear from our data that both the outflow and the radiation field associated with the stellar activity center are starting to disrupt it.

We would like to thank J. Bally and A. Lane for generously allowing us the use of their CO maps in advance for publication. We thank Alejandro Raga and Enrique Vázquez for valuable comments on hydrodynamical instabilities. We also thank our referee, G. Moriarty Schieven, for his review of the manuscript. We acknowledge the hospitality offered by the Harvard-Smithsonian Center for Astrophysics where part of the data reduction was made. P. T. P. H. is partially supported by NASA grant NAGW-3121. L. F. R. and J. C. acknowledge support from DGAPA-UNAM grants IN100589 and IN100291 and from CONACyT grant 0752-E9109. J. M. T. and L. V. are partially supported by SEUI (Spain) grant PB87-0371 and by Junta de Andalucía (Spain).

REFERENCES

Avery, L. W., Hayashi, S. S., & White, G. J. 1990, ApJ, 357, 542
Bally, J., & Lane, A. P. 1991, in Astrophysics with Infrared Arrays, ed. R. Elston (ASP Conf. Ser., 14), 273
———. 1992, private communication
Barral, J. F., & Cantó, J. 1981, Rev. Mexicana. Astron. Af., 5, 101
Cohen, R. J., Rowland, P. R., & Blair, M. M. 1984, MNRAS, 210, 425
Corcoran, D. 1991, private communication
Danby, G., Flower, D. R., Valiron, P., Schilke, P., & Walmsley, C. M. 1988, MNRAS, 235, 229
Estalella, R., Mauersberger, R., Torrelles, J. M., Anglada, G., Gómez, J. F., & López, R. 1992, ApJ, submitted
Evans, N. J., II, et al. 1981, ApJ, 244, 115
Garay, G., Moran, J. M., & Rodríguez, L. F. 1992, ApJ, submitted
Garay, G., & Rodríguez, L. F. 1990, ApJ, 362, 191
Garay, G., Rodríguez, L. F., & van Gorkom, J. H. 1986, ApJ, 309, 553
Goldsmith, D. F., & Langer, W. D. 1978, ApJ, 222, 881
Güsten, R., Chini, R., & Neckel, T. 1984, A&A, 138, 205
Gyulbudaghian, A. L., Glushkov, Yu, I., & Denisyuk, E. K. 1978, ApJ, 224, L137
Hartigan, P., & Lada, C. J. 1985, ApJS, 59, 383
Hartigan, P., Lada, C. J., Stocke, J., & Tapia, S. 1986, AJ, 92, 1155
Hayashi, S. S., Hasegawa, T., & Kaifu, N. 1988, ApJ, 332, 354
Herbst, E., & Klemperer, W. 1973, ApJ, 185, 505
Ho, P. T. P., Moran, J. M., & Rodríguez, L. F. 1982, ApJ, 262, 619
Ho, P. T. P., & Townes, C. H. 1983, ARA&A, 21, 239
Hughes, V. A. 1988, ApJ, 333, 788
———. 1989, AJ, 97, 1114
Hughes, V. A., & Moriarty-Schieven, G. 1990, ApJ, 360, 215
Hughes, V. A., & Wouterloot, J. G. A. 1982, A&A, 106, 171
———. 1984, ApJ, 276, 204
Johnson, H. L. 1957, ApJ, 126, 121
Joyce, R. R., & Simon, T. 1986, AJ, 91, 113
Keto, E. R., Ho, P. T. P., & Haschick, A. D. 1987, ApJ, 318, 712
Lada, C. J., Blitz, L., Reid, M. J., & Moran, J. M. 1981, ApJ, 243, 769
Lamb, H. 1932, in Hydrodynamics (Cambridge: Cambridge Univ. Press)
Lenzen, R. 1988, A&A, 190, 269
Lenzen, R., Hodapp, K.-W., & Solf, J. 1984, A&A, 137, 202
Loren, R. D., & Wootten, A. H. 1978, ApJ, 225, L81
Moriarty-Schieven, G. H., Snell, R. L., & Hughes, V. A. 1991, ApJ, 374, 169
Myers, P. C., Fuller, G. A., Goodman, A. A., & Benson, P. J. 1991, ApJ, 376, 561
Norris, R. P. 1980, MNRAS, 193, 39P
Rodríguez, L. F. 1989, in Structure and Dynamics of the Interstellar Medium (Berlin: Springer), 197
Rodríguez, L. F., & Cantó, J. 1983, Rev. Mexicana Astron. Af., 8, 163
Rodríguez, L. F., Cantó, J., Torrelles, J. M., & Ho, P. T. P. 1986, ApJ, 301, L25
Rodríguez, L. F., Ho, P. T. P., & Moran, J. M. 1980, ApJ, 240, L149
Sargent, A. I. 1977, ApJ, 218, 736
Scoville, N., & Kwan, J. 1976, ApJ, 206, 718
Shu, F. H. 1992, in the Physics of Astrophysics, Gas Dynamics (Mill Valley, CA: University Science Books)
Torrelles, J. M., Eiroa, C., Mauersberger, R., Estalella, R., Miranda, L. F., & Anglada, G. 1992, ApJ, 384, 528
Torrelles, J. M., Ho, P. T. P., Rodríguez, L. F., & Cantó, J. 1985, ApJ, 288, 595 (THRC85)
———. 1986, ApJ, 305, 721 (THRC86)
Torrelles, J. M., Rodríguez, L. F., Cantó, J., & Ho, P. T. P. 1993, ApJ, 404, L75, (TRCH93)
Torrelles, J. M., Rodríguez, L. F., Cantó, J., Carral, P., Marcaide, J. M., Moran, J. M., & Ho, P. T. P. 1983, ApJ, 274, 214
Walmsley, C. M., & Ungerechts, H. 1983, A&A, 122, 164
Wood, D. O. S., & Churchwell, E. 1989, ApJS, 69, 831